

# Synthesis of Compact Lumped Models From Electromagnetic Analysis Results

James C. Rautio, *Fellow, IEEE*

**Abstract**—Synthesis of compact lumped (*RLC*) models from the results of an electromagnetic (EM) analysis of planar circuits is described. The technique requires precise EM analysis *S*-parameter data at two or more frequencies. Data at up to five frequencies allows synthesis of more complicated models. For each port-to-port (i.e., “branch”) connection, 662 potential branch models are first synthesized and tested. Branch models that best match the EM results at all nonsynthesis frequencies are selected. For structures for which a compact lumped model is appropriate, this technique yields models that often provide direct physical insight into the electrical nature of the modeled structure. For electrically large structures, the technique is extended by the use of supplemental internal EM analysis ports. The technique is closed form; iteration is not used.

**Index Terms**—Compact models, electromagnetic (EM) analysis, lumped models, method of moments, model extraction, model-order reduction, model synthesis, reduced-order systems.

## I. INTRODUCTION

THERE HAS been significant work over several decades [1]–[23] with the goal of extracting a lumped model from numerical response data. Some of this work [2]–[9] involves various techniques that extract a pole-zero description from time and/or frequency domain data, sometimes requiring some form of iteration, optimization, or fitting. In addition, due to the distributed nature of the circuits being modeled, the model for even a simple circuit can become complicated with the resulting model bearing no physical resemblance to the circuit being modeled. The model is then effectively an abstract curve fitting with no direct correspondence to the physical structure being modeled. The advantage of these models is that extremely arbitrary circuits can be modeled over wide frequency ranges.

In other cases, a specialized model topology is selected and element values are extracted from measured or electromagnetic (EM) analysis data [1], [10]–[23]. In some cases, the element values give insight into the physical circuit being modeled.

A generalization of this second approach is described in this paper. While it is possible, using this generalized approach, to model a wide variety of circuits, it cannot be applied to every possible microwave circuit. Rather, it can be applied only to circuits that can be modeled within a specific (but large) set of physically appropriate lumped elements. The allowed circuit size can be made arbitrarily large by adding supplemental in-

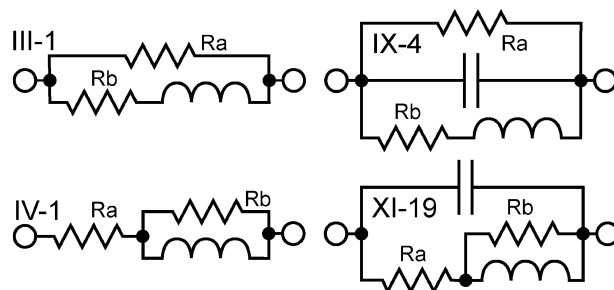


Fig. 1. Example branch models. Branch model IX-4 was used in my original lumped model synthesis effort. It is equivalent to XI-19, as can be seen after noting that the III-1 and IV-1 branch models are equivalent, as is discussed in the text.

ternal EM analysis ports (that facilitate the modeling process); however, the circuits selected for the model between each port (including the supplemental internal ports) must still come from within the allowed solution space.

The advantages of this approach are that the lumped models often correspond, element by element, to the circuit being modeled and that the resulting models tend to be especially compact. The approach involves no iteration of any kind. Typical synthesis time for a two-port circuit is less than 1 s using prototype software written in Visual BASIC macros on Microsoft Excel. Synthesis time increases with the number of ports squared. Production code will be compiled C++.

This paper begins with a detailed description of the technique, followed by a discussion of the effect of EM analysis error, an illustration of the need for negative valued elements, and closes with an example. In this study, I use the term “element” to denote an individual resistor, inductor, or capacitor. A “branch” or “branch model” is a two-terminal collection of elements for connection between two nodes. Ground is considered to be a node. A “model” is a collection of branch models forming a nodal network.

## II. DESCRIPTION OF THE TECHNIQUE

The synthesis technique described here is a generalization of [1], where an  $N$ -port circuit is analyzed electromagnetically at two frequencies. The result is converted to *Y*-parameters from which the admittance connecting each node (i.e., port) is calculated.

Next, the IX-4 branch model in Fig. 1 is synthesized from the resulting admittance data. There are four unknown elements ( $R_A$ ,  $R_B$ ,  $L$ , and  $C$ ). We write the expression for the admittance of this branch model, and given the real and imaginary admittance data at two frequencies, we generate four simultaneous equations. The equations are nonlinear, but they do possess a so-

lution. In [1], an approximate solution was presented. The exact synthesis is

$$\frac{L}{R_B} = \frac{\omega_2 b_1 - \omega_1 b_2}{\omega_1 \omega_2 (g_2 - g_1)} \quad (1)$$

$$R_B = \frac{(\omega_2^2 - \omega_1^2) (L/R_B)^2}{(g_1 - g_2) (1 + \omega_1^2 (L/R_B)^2) (1 + \omega_2^2 (L/R_B)^2)} \quad (2)$$

$$\frac{1}{R_A} + j\omega_1 C = y_1 - \frac{1}{R_B + j\omega_1 L}. \quad (3)$$

Numeric subscripts indicate data from one of the two synthesis frequencies with the node-to-node admittance being  $y = g + jb$ , and  $\omega$  being the radian frequency. The model is passive if  $R_A \geq 0$  and  $1/R_B \geq -1/R_A$ . It is stable if  $L$  has the same sign as  $R_B$ , and  $LC$  has the same sign as  $1 + R_B/R_A$ , and  $1/R_A C \geq -R_B/L$ . Note that negative elements are allowed in a branch model that is both passive and stable.

If one or more of the four elements are close to 0, then the branch is simplified. For example, if  $1/R_A$  and  $C$  are close to 0, we have a series  $RL$ . This process is repeated for all possible node-to-node (and node-to-ground) connections. For each node-to-node admittance, a lumped equivalent circuit is synthesized and the model supplemented.

The problem is that there are numerous branch models that might be needed, but cannot be represented as a special case of the IX-4 branch model. For example, two two-element branch models (series  $RC$  and series  $LC$ ), and numerous three-element branch models are left unconsidered. In this new approach, every possible zero-, one-, two-, three-, and four-element branch model is synthesized. Many five-, six-, seven-, and eight-element branch models are also synthesized. Based on comparison with EM analysis data not used for synthesis, the best branch model to represent the EM analysis result is then selected.

We presently synthesize 662 candidate branch models (this includes different ways of synthesizing the same branch model) for each node-to-node connection in a given  $N$ -port. Thus, for a two-port, which has three node-to-node connections (ground is a node), we consider  $662^3$  potential models, and of these we select the model that best matches the EM analysis results at the nonsynthesis frequencies. Thus, we select the best possible model from a comprehensive solution space of 290 117 528 potential models for a two-port.

This new approach allows an efficient automation of compact model generation. Performed manually, a designer proposes a lumped model. By some combination of calculation, guessing, and optimization, the designer determines if that model can then adequately represent the EM results. If not, then the designer speculatively selects another compact lumped model and repeats the tedious extraction and evaluation. With existing model extraction techniques, the best compact model is highly unlikely to be found and compact model generation cannot be automated because of the high degree of skill required, a computer cannot replace the engineer. In this approach, a new technique synthesizes and evaluates hundreds of millions of models with selection of the best model taking place in real time.

### III. CANDIDATE BRANCH TOPOLOGIES

There is one possible zero-element topology, a single one-element topology, two two-element topologies, four three-element

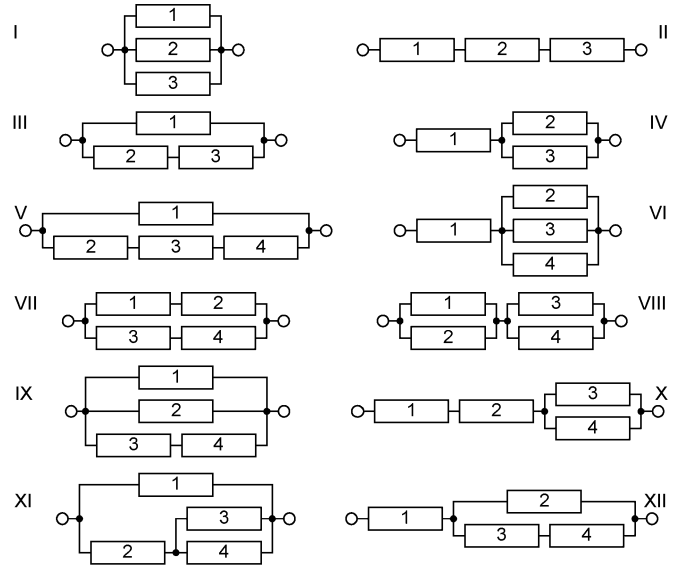


Fig. 2. There are four possible three-element branch topologies and eight possible four-element topologies. The elements are ordered as indicated.

topologies, and eight four-element topologies. All possible three- and four-element topologies are shown in Fig. 2.

Each topology has a final element connection. The final connection for all the odd-numbered (Roman numeral) topologies is in parallel and it is thus most convenient to write an equation for admittance. The final connection for all even-numbered topologies is in series. Now we most conveniently write an equation for impedance.

Note that the next higher even-numbered (Roman numeral) topology represents the dual (i.e., swap  $L$  and  $C$ , and swap parallel and series connections) for each odd-numbered topology. Thus, when synthesis equations are derived for a type-III topology, we immediately have the solution for a type-IV topology with the changes: 1) swap  $L$  and  $C$ ; 2) invert  $R$ ; and 3) swap impedance and admittance. Thus, synthesis equations need be derived for only half of the branch models.

Table I shows how each of the three- and four-element topologies are populated. For example, a type III-1 branch model (Fig. 1) is a resistor in parallel with a series connected resistor and inductor. This is indicated by the entry “1  $RRL$ ” under the heading “III, IV.” Branch model elements are listed in a specific order:  $R, L$ , and  $C$  are arbitrarily considered to be in smallest to largest order (as in “1, 2, 3”). The element populations are ordered in Table I as though they are in numeric order. Thus,  $RRC$  immediately follows  $RRL$ , etc.

The first (most significant) element is assigned to element 1 (always an element involved in the final connection) in Fig. 2, etc. For example, branch model IV-7 is a  $CRL$ . Thus, element 1 (in topology IV of Fig. 2) is a capacitor, element 2 is a resistor, and element 3 is an inductor.

The zero-, one-, and two-element topologies are not assigned numerical designations; rather we simply use their common names, e.g., “Series  $RC$ ,” etc.

There are two zero-element branch models (an open and short circuit), three one-element branch models, six two-element branch models, 20 three-element branch models, and 90

TABLE I  
BRANCH MODEL SPECIFICATION

I, II	VII, VIII	XI, XII	XI, XII
1 RLC	1 RLRL	1 RRRL	18 LCLC
III, IV	2 RLRC	2 RRRC	19 CRRL
	3 RLLC	3 RRLC	20 CRRC
1 RRL	4 RCRC	4 RLRL	21 CRCL
2 RRC	5 RCLC	5 RLRC	22 CLRL
3 RLC	6 LCLC	6 RLLC	23 CLRC
4 LRL	IX, X	7 RCRL	24 CLLC
5 LRC		8 RCRC	25 CCRL
6 LLC	1 RLRL	9 RCLC	26 CCRC
7 CRL	2 RLRC	10 LRRR	27 CCLC
8 CRC	3 RLLC	11 LRRR	
9 CLC	4 RCRL	12 LRLC	
V, VI	5 RCRC	13 LLRL	
	6 RCLC	14 LLRC	
	7 LCRL	15 LLLC	
1 RRLC	8 LCRC	16 LCRL	
2 LRLC	9 LCLC	17 LCRC	
3 CRCL			

four-element branch models, for a total of 121 possible branch models of up to four elements.

#### IV. EQUIVALENCES BETWEEN BRANCH MODELS

A number of the branch models are equivalent. This means that given the values for either branch model, the other branch model can be uniquely determined. The impedance of both branch models is identical at all frequencies. For example, Fig. 1 shows branch models III-1 and IV-1. That equivalence exists is seen by inspection. The only difference between the two branch models is the location where the parallel connected resistor is tapped into the series-connected resistor. The resistor and inductor values can be selected so that both branches have exactly the same impedance at all frequencies.

The three-element equivalences are useful in identifying four-element equivalences. For example Fig. 1 also shows the XI-19 branch model. Noting that this is IV-1 with a capacitor connected in parallel, we have IX-4 of Fig. 1 by changing the IV-1 portion to the equivalent III-1 branch model. It is instructive to fill in a similar table with the schematics of each equivalent branch model. Patterns quickly emerge, such as described above. Space limits do not permit presentation of such a table here.

In this approach, we synthesize all possible branch models, even if there are equivalences, because one branch model might have more desirable element values or yield a better fit to actual data. In fact, in some cases, one branch model might have all positive element values while the equivalent branch model has some negative values.

Take, for example, the first line of Table II. An III-1 is equivalent to an IV-1, as described above. In addition, it is also equivalent to an III-2. This seems counter-intuitive because the III-1 is an inductor embedded in a resistive network, while III-2 is a capacitor similarly embedded. Note that III-1 is not listed in boldface, while III-2 is bold. This indicates that if one of the branch models has all positive elements, the other must have

TABLE II  
BRANCH MODEL EQUIVALENCES

III-1	III-2	IV-1	IV-2	XI-1	XI-2	XII-1	XII-2
III-4	IV-4	XI-13	XII-13				
III-6	IV-6	XI-15	XII-15				
III-8	IV-8	XI-26	XII-26				
III-9	IV-9	XI-27	XII-27				
V-1	<b>VI-1</b>	<b>XI-3</b>	XII-3				
V-2	XII-14						
V-3	XII-25						
VI-2	XI-14						
VI-3	XI-25						
VII-1	X-1	<b>X-2</b>	XII-4	XII-10	<b>XII-11</b>		
VII-4	<b>X-4</b>	X-5	XII-8	<b>XII-19</b>	XII-20		
VII-6	X-9	XII-18	XII-24				
VIII-1	IX-1	<b>IX-2</b>	XI-4	XI-10	<b>XI-11</b>		
VIII-4	<b>IX-4</b>	IX-5	XI-8	<b>XI-19</b>	XI-20		
VIII-6	IX-9	XI-18	XI-24				
IX-3	XI-6						
IX-6	XI-9						
IX-7	XI-22						
IX-8	XI-17						
X-3	XII-6						
X-6	XII-9						
X-7	XII-22						
X-8	XII-17						

Branch models in each row are equivalent. Bold face indicates some elements are negative when the nonbold-faced branch models are all positive. The XI and XII branch models in the first five rows are not equivalences, rather, they reduce to the three-element branch models on the same row.

some negative elements. Indeed, the equivalence from III-1 to III-2 is

$$R'_A = R_A R_B / (R_A + R_B) \quad R'_B = -R_B \quad C' = -L / R_B^2 \quad (4)$$

where the prime indicates the III-2 element value. Equivalence equations have been derived for many, but not all, of the listed equivalences. We determine equivalence by noting that the impedance or admittance equations have the same form and by comparing numerical results for a specific case of one branch model synthesized from data generated by the other branch model.

We do not synthesize 12 of the four-element branch models because they reduce to three-element branch models. These are the XI and XII branch models listed in the first five lines of Table II. Thus, 108 branch models of up to four elements are synthesized. Strictly speaking, these four-element branch models are not equivalent to the three-element branch models even though element values can be selected that yield identical impedance at all frequencies. The reason is that given a specific three-element branch model, one cannot uniquely determine the corresponding four-element branch model; there are an infinite number of solutions.

There are no equivalences for branch models with fewer than three elements. All three- and four-element equivalences are summarized in Table II. All the lossless equivalences have been previously reported [24]. We expect these equivalences to be useful for filter and matching network synthesis. Numerous equivalences between branch models of up to eight elements have been observed and are not reported here.

## V. SYNTHESIS STRATEGIES

Each synthesis derivation starts by writing an expression for the admittance (parallel final connection) or impedance (series final connection). Sometimes both admittance and impedance expressions can be used to give additional synthesis opportunities. The resulting expression is split into real and imaginary parts. If one is writing the expression for the admittance of a branch model, it is split into two expressions, one for conductance ( $g$ ) and another for susceptance ( $b$ ).

In the first strategy, one takes EM data at a sufficient number of frequencies and writes an equation for both the real and imaginary parts at each frequency. For example, when synthesizing a three-element branch model, we require three equations. With data at two frequencies, we have two equations for conductance and two equations for susceptance. This forms a set of four nonlinear simultaneous equations. We select three equations (the fourth equation is satisfied only if we happen to synthesize the correct model for the data) and find an algebraic solution. This is the strategy used for the synthesis of IX-4 above. In some cases, the solution involves multiple roots. Every root must be evaluated and the resulting branch model considered.

In the second strategy, only the imaginary part of the admittance or impedance is used. A three-element branch model now requires data from three frequencies. In the third strategy, only the real part is used. The second strategy cannot be used for any branch model whose susceptance (or reactance) is unmodified by one or more elements. Likewise, the third strategy cannot be used for any branch model whose conductance (or resistance) is unmodified by one or more elements. For example, a parallel  $RC$  cannot be synthesized based only on the branch model's conductance or only on its susceptance, but it can be synthesized based only on its resistance or only on its reactance.

If the second strategy is used, additional branch models can be synthesized. For example, note that a resistor added in parallel to a branch model has no effect on the resulting susceptance. Thus, if a branch model is synthesized based only on its susceptance, we may now use the conductance to determine a resistor connected in parallel and add one more element to the synthesized branch model. Likewise, if reactance is used to synthesize a branch model, a resistor can be added in series with the branch model. Thus, for each branch model that can be synthesized using the second strategy, one more branch model with an additional resistor can also be synthesized.

If the third strategy is used, we can increase the complexity of the synthesized branch model by adding any lossless branch model. For example, if the synthesis is based on conductance only, we can add any lossless branch model in parallel and leave the conductance unchanged. The added lossless branch model is synthesized based on the unused susceptance information. The dual situation benefits a synthesis based only on resistance. The branch model complexity can be increased by synthesizing a lossless branch model based on the unused reactance information. There are 16 lossless branch models of up to four elements that can be added in this manner. Thus, for every branch model that can be synthesized using the third strategy, another 16 branch models can be synthesized of up to eight elements.

Branch models should be synthesized in all ways possible. This is because one synthesis strategy might be sensitive to difficulties that are transparent to another synthesis. For example, synthesis of a low-loss resonant branch model might have difficulties if based only on the real part of the impedance or admittance data.

The combination of all possible synthesis strategies applied to all possible zero- through four-element branch models (yielding branch models of up to eight elements) provides 662 candidate branch models for every node-to-node connection. As a practical matter, minimum and maximum limits should be set on the allowed values of all lumped elements. For example, a capacitor whose value is below a specified minimum limit should be treated as an open circuit. This significantly reduces the complexity of the resulting model in that high impedance shunt and low impedance series elements do not clutter the model. In addition, the limits can be used to adjust the model complexity and accuracy as desired.

## VI. SYNTHESIS ERROR CONSIDERATIONS

A great deal of effort has been expended over the years to extract lumped models that are causal, passive, and stable. If one were to have exact EM data for a causal, passive, stable structure and an extracted model that exactly matches the EM data, then the model must be causal, passive, and stable. Thus, models that are not causal, stable, or passive must be the result of some combination of EM analysis error and extraction/synthesis error.

The technique reported here can result in nonpassive unstable models when the structure is unsuitable for a compact lumped model within the technique's solution space at the selected synthesis frequencies. Typically, this is the result when a structure has a large distributed component. When this technique fails to provide an adequate model, any of the more general model extraction techniques, mentioned in Section I, should be used. A model that is inadequate for the structure being modeled is a failure due to extraction/synthesis error.

It has been my observation that even minor changes in EM data can result in large differences in the quality of the synthesized model. Thus, this technique is not especially useful for measured data due to measurement noise. All of my EM synthesis efforts use  $S$ -parameters evaluated to full double precision. If the same  $S$ -parameter data is truncated to the reduced precision common in  $S$ -parameter data files (the old-style "Touchstone" format), then substantially degraded models can result.

The EM analysis used in this study, i.e., [25] and [26], typically has over 100 dB of dynamic range [27], [28]. In addition, the EM analysis uses an exact deembedding algorithm [29], [30]. By "exact" we mean that provided the deembedding assumptions are not violated (i.e., no over-moded port connecting lines), then the port discontinuities are removed to within the numerical precision of the underlying EM analysis. There is no deembedding error added on top of the already existing EM analysis error.

EM deembedding algorithms that require knowledge of the characteristic impedance of the port connecting lines are typically not exact for inhomogeneous or lossy geometries due to

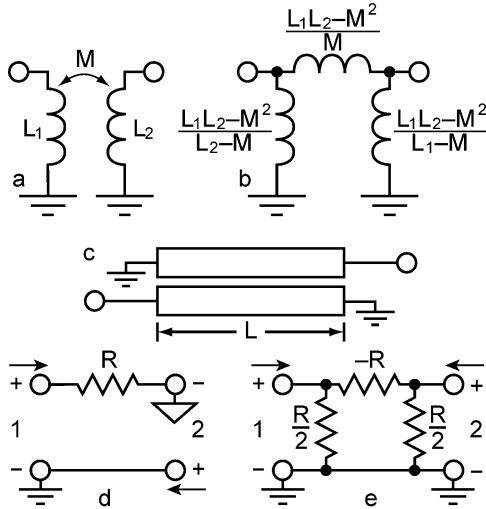


Fig. 3. Negative valued element situations. The circuits for *a*, *c*, and *d* require use of negative valued elements in their  $\pi$ -models.

ambiguity in characteristic impedance definitions. We suggest that nonpassive and unstable models extracted from such EM data might be the direct result of the very small, but nonphysical error introduced by the deembedding due to lack of knowledge of the exact characteristic impedance.

This problem is especially clear for causality. For lossy transmission lines, characteristic impedance is complex (as in real and imaginary). In order for a system to be causal, the magnitude and phase of the characteristic impedance must be related by a Hilbert transform [31]. Use of any characteristic impedance that is not causal (e.g., a pure real characteristic impedance for a lossy line) results in noncausal  $S$ -parameters. Even if a model extraction forces causality, then the noncausality of the  $S$ -parameter data could make itself known in some other way, perhaps as an unstable or nonpassive model.

In our approach, all characteristic impedances used are causal [30], the deembedding error is 0, and the dominant source of EM analysis error is error due to finite subsection size [27], [28]. It is our experience that error due to subsection size does not impact the stability or passivity of the resulting models. Rather, the percent error translates directly into percent error of the value of the dominant elements in a model. Typically, the subsection error (i.e., error due to meshing the circuit for EM analysis) is around 1% or less and is easily quantified.

## VII. NEGATIVE ELEMENT CONSIDERATIONS

When a nonpassive unstable model, for whatever cause, is a common extraction result, one can compensate by requiring all element values to be positive. This is a common, but unacceptable model restriction because certain situations require negative elements.

Fig. 3(a) shows coupled inductors and Fig. 3(b) shows the equivalent  $\pi$ -model. When  $M$  is negative, a negative inductor (between the two nodes) is required. The negative inductor can be hidden by use of a phase reversing transformer or a controlled source, but the negative inductor is still there.

In a similar example, Fig. 3(c) shows a coupled line. At low frequency (i.e., the length  $L$  of the line is short compared to

wavelength), there is a mutual inductance between the two lines. The circuit theory  $Y_{21}$  is inversely proportional to  $\sinh(\gamma L)$ . Using the small angle approximation ( $\gamma L$  small), we have the impedance between ports 1 and 2 proportional to  $-\gamma L = -(\alpha + j\beta)L$  with the sign resulting from conversion of the  $Y$ -parameter to the node-to-node connecting admittance. Notice that for a lossless situation ( $\alpha = 0$ ), the node-to-node impedance,  $-j\beta L$ , requires a negative inductor (a positive capacitor has the wrong frequency variation). For the lossy situation, the node-to-node impedance also includes a negative resistance  $-\alpha L$ . Thus, in order to model forward coupled crosstalk, negative elements are required.

Another situation is the interface between two circuits that do not share a perfect common ground. This could be the case with two connected circuits that simply have different grounds, or a circuit with a single resistive ground (e.g., silicon). A model is shown in Fig. 3(d). Ports 1 and 2 each have different ground references. Voltage placed across port 1 results in current flowing out of the ground terminal on port 2. The  $Y$ -parameters for this circuit are

$$\mathbf{Y} = \begin{bmatrix} 1/R & 1/R \\ 1/R & 1/R \end{bmatrix}. \quad (5)$$

This yields the  $\pi$ -model of Fig. 3(e), including a negative resistor. The stability and passivity of individual branches are not required for a complete model to be passive and stable. This situation also arises when modeling the interaction (perhaps for signal integrity purposes) between two different circuits, each using its own ground, and a signal on one circuit can induce current in the ground of the other circuit.

Notice that while the circuits of Fig. 3(d) and (e) are exactly equivalent no matter what termination is attached to ports 1 and 2, the same is not true if one were to add circuitry connecting nodes 1 and 2 together. For this reason, a model that contains multiple grounds that is later used within a larger circuit, nodal connections should be made *only* between nodes that are all referenced to exactly the same ground. This rule is sometimes violated when RF circuits on silicon are simulated by connecting together individual components available in a process design kit (PDK). The ports of the components in the PDK might have different ground references.

Thus, *inclusion of negative valued elements in a lumped model is required for modeling a wide range of circuits*, whether it is done on a general and explicit basis, as described here, or on a hidden basis that is limited to special situations, e.g., by including phase-reversing transformers. Since negative elements are required for maximum generality, passivity and stability cannot be enforced by restricting the model to positive elements. The only alternative is to use high-quality noise-free EM data.

## VIII. EXAMPLE SYNTHESIS

To illustrate this model synthesis approach, a six-turn circular spiral inductor on silicon has been selected, and a scale image is inset into Fig. 4. The linewidth is  $10 \mu\text{m}$  and the gap is  $2 \mu\text{m}$ . It is on top of  $10 \mu\text{m}$  of lossless  $\epsilon_R = 4.0$  dielectric, which itself is on top of  $100 \mu\text{m}$  of silicon ( $\epsilon_R = 11.9$ , conductivity =  $1.0 \text{ S/m}$ ). The inside end of the spiral passes

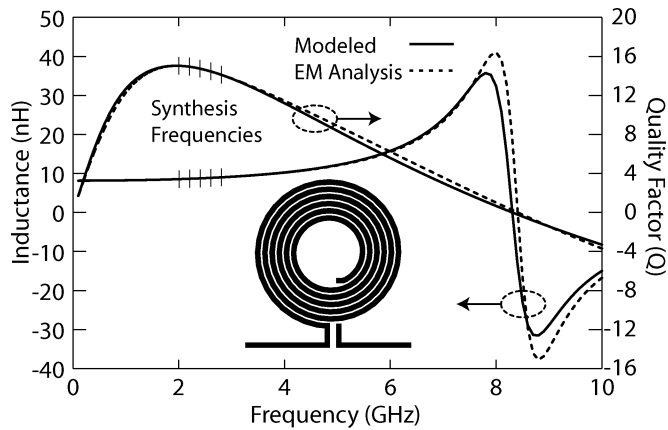


Fig. 4. Modeled data from the circuit in Fig. 5. The model was synthesized from the EM analysis data at the indicated frequencies.

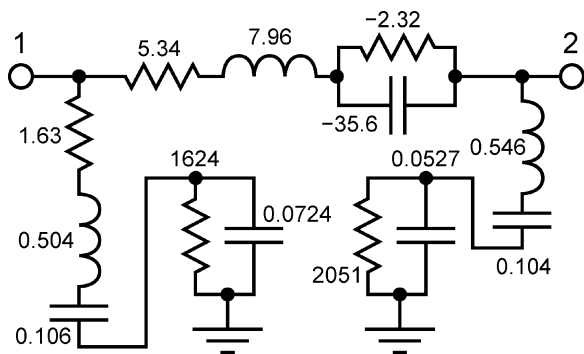


Fig. 5. Synthesized compact model for a spiral inductor on silicon shows the physical inductor (7.96 nH) and associated circuitry modeling the multiple loss mechanisms. Units are ohms ( $\Omega$ ), nanohenrys (nH), and picofarads (pF).

out  $4 \mu\text{m}$  underneath the spiral. Analysis reference planes are located at the start of the vertical segment of feed line. The cell size is  $2\text{-}\mu\text{m}$  square and the box size is  $500\text{-}\mu\text{m}$  square. Conformal meshing [32] is used for the circular portion of the spiral. The small cell size allows high edge current. Metal thickness is not included, as it is not needed for validation of this synthesis. The inductor was analyzed electromagnetically from 0.1 to 10 GHz. The model was synthesized from the EM data at five evenly spaced frequencies from 2.0 to 2.8 GHz.

The inductance of the spiral itself is the 7.96-nH inductor in the schematic of Fig. 5. Much of the additional complexity of the model is due to skin-effect resistance (present in both the metal of the spiral and the silicon substrate). Lumped resistors do not vary with the square root of frequency. In addition, the metal loss has a very complicated frequency dependence [33] that is also not modeled by frequency-independent resistors.

The model includes two negative elements. A pole-zero SPICE analysis<sup>1</sup> shows all poles and zeros are stable and a transient analysis does, in fact, converge nicely. In addition, note that the series arm is a X-2 branch model, equivalent (Table II) to, among others, the X-1 with all positive element values, and thus, the model is passive and stable.

In [13]–[16], various combinations of a pair of coupled inductors with a resistor across the terminals of one inductor are used

to model the series arm of a spiral inductor. That four-parameter branch model reduces to the three-element IV-4 branch model. The idea is to increase resistance as the frequency increases. Note that a portion of the series arm branch model synthesized here (Fig. 5) resembles an IV-4 only with a negative parallel RC instead of a positive parallel RL. This configuration effectively decreases resistance as frequency decreases.

The inductors in the shunt branches have been seen in the synthesis of a wide variety of spiral inductors using this technique. We suggest that these inductances might actually be physical, as opposed to an abstract curve-fitting artifact, and are perhaps due to the inductance of the ground return current flowing in the surface of the silicon. The shunt arms of the model include the IV-8 branch model often used for this purpose in spiral inductor modeling. The parallel RC models the resistance and capacitance of the silicon substrate, while the series capacitor models the capacitance of the lossless dielectric between the spiral and silicon.

When this study was initially submitted, [23] reported use of the X-2 branch model (which includes a series inductor) to model the shunt arms of a spiral inductor model, and the X-2 branch model in parallel with a series RL is to model the series arm. The resistor in parallel with the capacitor in [23] is sometimes negative, and [23] reported that conservation of energy is not violated, however, stability is not discussed. Use of the III-1 branch model (Fig. 1) for spiral inductor compact modeling is reported in [10]–[12]. The III-7 branch model combined with a parallel RC is used in [17]–[19]. The X-2 branch model, combined with coupled inductors, is used to build general models in [9].

Modeled versus EM analysis results are shown in Fig. 4 with synthesis frequencies indicated. The inductor resonance and high-frequency  $Q$  are well modeled even though the synthesis frequencies are far below resonance.

Models for numerous circuits have been synthesized. We have successfully synthesized lossless and metal loss only spiral inductors based on EM data at very low frequencies with results valid far above resonance. Lengths of transmission line have in some cases been successfully synthesized well above one half-wavelength in length yielding simple pure lumped models, a most unexpected result. Simple pure lumped broadband models for antennas have been synthesized. In research to be reported in the future, we can now synthesize ideal transmission lines, multiple coupled lines, and  $N$ -port tee networks.

Compact model extraction of coupled lines from EM data is described in [20], however, they “calibrate” the EM analysis to match measurements by significant adjustments to the EM analysis substrate conductivity, making the analyzed substrate conductivity significantly different from that measured at dc. This approach is dangerous because a common measurement flaw can masquerade as modified substrate conductivity [34].

A patent on this compact model synthesis technique has been submitted.

## IX. CONCLUSION

A technique to synthesize a lumped model based on high-quality EM analysis data has been described. All possible combinations of resistors, inductors, and capacitors up to a certain

<sup>1</sup>[Online]. Available: <http://www.aimspice.com>

level of complexity have been synthesized from the EM data. The branch models that best match the EM analysis data at all nonsynthesis frequencies have then been selected for the model. Using this approach, the best of literally hundreds of millions of possible models have been selected. If there exists a compact lumped model within the synthesis solution space that can model a given structure, then this technique finds that model.

## REFERENCES

- [1] J. C. Rautio, "Synthesis of lumped models from  $N$ -port scattering parameter data," *IEEE Trans. Microw. Theory Tech.*, vol. 42, no. 3, pp. 535–537, Mar. 1994.
- [2] A. Kogure, "Automatic SPICE models and  $S$ -parameters analysis," (in Japanese) *Design Wave Mag.*, no. 20, pp. 145–151, Mar. 1999.
- [3] I. Timmins and K. L. Wu, "An efficient systematic approach to model extraction for passive microwave circuits," *IEEE Trans. Microw. Theory Tech.*, vol. 48, no. 9, pp. 1565–1573, Sep. 2000.
- [4] S. D. Corey and A. T. Yang, "Automatic netlist extraction for measurement-based characterization of off-chip interconnect," *IEEE Trans. Microw. Theory Tech.*, vol. 45, pp. 1934–1940, Oct. 1997.
- [5] R. Araneo, "Extraction of broadband passive lumped equivalent circuits of microwave discontinuities," *IEEE Trans. Microw. Theory Tech.*, vol. 54, no. 1, pp. 393–401, Jan. 2006.
- [6] R. Neumayer, A. Stelzer, F. Haslinger, and R. Weigel, "On the synthesis of equivalent-circuit models for multiports characterized by frequency-dependent parameters," *IEEE Trans. Microw. Theory Tech.*, vol. 50, no. 12, pp. 2789–2796, Dec. 2002.
- [7] L. F. Tiemeijer, R. J. Havens, R. De Kort, Y. Bouttelement, P. Deixler, and M. Ryzek, "Predictive spiral inductor compact model for frequency and time domain," in *IEEE Int. Electron Devices Meeting Tech. Dig.*, Dec. 2003, pp. 36.4.1–36.4.4.
- [8] S. Sercu and L. Martens, "A new algorithm for experimental circuit modeling of interconnection structures based on causality," *IEEE Trans. Compon., Packag., Manuf. Technol. B*, vol. 19, no. 2, pp. 289–295, May 1996.
- [9] T. Mangold and P. Russer, "Full-wave modeling and automatic equivalent circuit generation of millimeter-wave planar and multilayer structures," *IEEE Trans. Microw. Theory Tech.*, vol. 47, no. 6, pp. 851–858, Jun. 1999.
- [10] T. Kamgaing, M. Petras, and M. Miller, "Broadband compact models for transformers on conductive silicon substrates," in *IEEE Radio Freq. Integrated Circuits Symp.*, 2004, pp. 457–460, Paper TU1D-4.
- [11] T. Kamgaing, T. Meyers, M. Petras, and M. Miller, "Modeling of frequency dependent losses in two-port and three-port inductors on silicon," in *IEEE Radio Freq. Integrated Circuits Symp.*, Jun. 2002, pp. 307–310, Paper TU3A-2.
- [12] T. Kamgaing, T. Meyers, M. Petras, and M. Miller, "Modeling of frequency dependent losses in two-port and three-port inductors on silicon," in *IEEE MTT-S Int. Microw. Symp. Dig.*, 2002, pp. 153–156, Paper TU3A-2.
- [13] D. Melendy, P. Francis, C. Pichler, K. Hwang, G. Srinivasan, and A. Weisshaar, "A new wideband compact model for spiral inductors in RFICs," *IEEE Electron Device Lett.*, vol. 23, no. 5, pp. 273–275, May 2002.
- [14] A. Watson, Y. Mayevskiy, P. Francis, K. Hwang, G. Srinivasan, and A. Weisshaar, "Compact modeling of differential spiral inductors in Si-based RFICs," in *IEEE MTT-S Int. Microw. Symp. Dig.*, 2004, pp. 1053–1056, Paper WE1F-7.
- [15] Y. Mayevskiy, A. Watson, P. Francis, K. Hwang, and A. Weisshaar, "A new compact model for monolithic transformers in silicon-based RFICs," *IEEE Microw. Wireless Compon. Lett.*, vol. 15, no. 6, pp. 419–421, Jun. 2005.
- [16] A. Watson, D. Melendy, P. Francis, K. Hwang, and A. Weisshaar, "A comprehensive compact-modeling methodology for spiral inductors in silicon-based RFICs," *IEEE Trans. Microw. Theory Tech.*, vol. 52, no. 3, pp. 849–857, Mar. 2004.
- [17] K. Naishadham, "Experimental equivalent-circuit modeling of SMD inductors for printed circuit applications," *IEEE Trans. Electromagn. Compat.*, vol. 43, no. 4, pp. 557–56, Nov. 2001.
- [18] K. Naishadham, "Measurement-based closed-form modeling of surface-mounted RF components," *IEEE Trans. Microw. Theory Tech.*, vol. 50, no. 10, pp. 2276–2286, Oct. 2002.
- [19] J. Sieiro, J. M. López, J. Cabanillas, J. A. Osorio, and J. Samitier, "A physical frequency-dependent compact model for RF integrated inductors," *IEEE Trans. Microw. Theory Tech.*, vol. 50, no. 1, pp. 384–392, Jan. 2002.
- [20] T. Kim, X. Li, and D. J. Allstot, "Compact model generation for on-chip transmission lines," *IEEE Trans. Circuits Syst. I, Reg. Papers*, vol. 51, no. 3, pp. 459–470, Mar. 2004.
- [21] A. Lauer and I. Wolff, "A conducting sheet model for efficient wide band FDTD analysis of planar waveguides and circuits," in *IEEE MTT-S Int. Microw. Dig.*, Jun. 2000, vol. 1, pp. 255–258.
- [22] M. Ingalls and G. Kent, "Measurement of the characteristics of high- $Q$  ceramic capacitors," *IEEE Trans. Compon., Hybrids, Manuf. Technol.*, vol. CHMT-12, no. 4, pp. 487–495, Dec. 1987.
- [23] K. Y. Lee, S. Mohammadi, P. K. Bhattacharya, and L. P. B. Katehi, "A wideband compact model for integrated inductors," *IEEE Microw. Wireless Compon. Lett.*, vol. 16, no. 9, pp. 490–492, Sep. 2006.
- [24] A. I. Zverev, *Handbook of Filter Synthesis*. New York: Wiley, 1967, pp. 522–527.
- [25] J. C. Rautio and R. F. Harrington, "An electromagnetic time-harmonic analysis of shielded microstrip circuits," *IEEE Trans. Microw. Theory Tech.*, vol. MTT-35, no. 8, pp. 726–730, Aug. 1987.
- [26] J. C. Rautio, "A time-harmonic electromagnetic analysis of shielded microstrip circuits," Ph.D. dissertation, Dept. Elect. Comput. Eng., Syracuse Univ., Syracuse, NY, 1986.
- [27] J. C. Rautio, "An ultrahigh precision benchmark for validation of planar electromagnetic analyses," *IEEE Trans. Microw. Theory Tech.*, vol. 42, no. 11, pp. 2046–2050, Nov. 1994.
- [28] J. C. Rautio, "Testing limits of algorithms associated with high frequency planar electromagnetic analysis," in *Proc. 33rd Annu. Eur. Microw. Conf.*, Munich, Germany, 2003, pp. 463–466.
- [29] J. C. Rautio, "A de-embedding algorithm for electromagnetics," *Int. J. Microw. Millimeter-Wave Comput.-Aided Eng.*, vol. 1, no. 3, pp. 282–287, Jul. 1991.
- [30] J. C. Rautio and V. I. Okhmatovski, "Unification of double-delay and SOC electromagnetic deembedding," *IEEE Trans. Microw. Theory Tech.*, vol. 53, no. 9, pp. 2892–2898, Sep. 2005.
- [31] D. F. Williams, B. K. Alpert, U. Arz, D. K. Walker, and H. Grabinski, "Causal characteristic impedance of planar transmission lines," *IEEE Trans. Adv. Packag.*, vol. 26, no. 2, pp. 165–171, May 2003.
- [32] J. C. Rautio, "A conformal mesh for efficient planar electromagnetic analysis," *IEEE Trans. Microw. Theory Tech.*, vol. 52, no. 1, pp. 257–264, Jan. 2004.
- [33] J. C. Rautio and V. Demir, "Microstrip conductor loss models for electromagnetic analysis," *IEEE Trans. Microw. Theory Tech.*, vol. 51, no. 3, pp. 915–921, Mar. 2003.
- [34] J. C. Rautio and R. Groves, "A potentially significant on-wafer high-frequency measurement calibration error," *IEEE Micro*, pp. 94–100, Dec. 2005.



**James C. Rautio** (S'77–M'78–SM'91–F'00) received the B.S.E.E. degree from Cornell University, Ithaca, NY, in 1978, the M.S. degree in systems engineering from the University of Pennsylvania, Philadelphia, in 1982, and the Ph.D. degree in electrical engineering from Syracuse University, Syracuse, NY, in 1986.

From 1978 to 1986, he was with General Electric, initially with the Valley Forge Space Division, then with the Syracuse Electronics Laboratory. During this time, he developed microwave design and measurement software and designed microwave circuits on alumina and on GaAs. From 1986 to 1988, he was a Visiting Professor with Syracuse University and Cornell University. In 1988, he joined Sonnet Software, Liverpool, NY, full time, a company he had founded in 1983. In 1995, Sonnet Software was listed on the Inc. 500 list of the fastest growing privately held U.S. companies, the first microwave software company ever to be so listed. Today, Sonnet Software is the leading vendor of 3-D planar high-frequency EM analysis software.

Dr. Rautio was the recipient of the 2001 IEEE Microwave Theory and Techniques Society (IEEE MTT-S) Microwave Application Award. He was appointed an MTT-S Distinguished Microwave Lecturer for 2005–2007 lecturing on the life of James Clerk Maxwell.